

PERFORMANCE OF PLUG -TYPE ROCKET EXHAUST

Pires, M.,manoloneuzalucas@yahoo.com.br

Fifthvision Technology Research and Development- Av. Brig. Faria Lima, 1699 –Jd Flamboyant – São José dos Campos- SP

Nobres, N. D.,Instituto Militar de engenharia-IME - Av. Gen. Tibúrcio s/n Praia vermelha-Rio de Janeiro-RJ

Abstract. This paper discusses the theoretical analysis of axisymmetrical supersonic flows in conventional and no conventional nozzles (plug nozzles) and makes a comparative analysis between these nozzles for their main parameter (thrust coefficient) under several operational conditions. Characteristics of Plug nozzle flow fields are discussed based on the results of numerical simulations. The mathematical formulation obtained through this theoretical analysis is solved numerically. Basic control equations and characteristic equations (Mach lines) are deduced. The transonic flow region is also analyzed. An equation for an initial-value line is developed together with the parameters along this line. The system of differential equations formed by the compatibility valid along the characteristics is solved from its initial-value line. This is solved numerically using characteristics method. The numerical results show that a better performance of the plug nozzles is obtained under over expansion conditions. This comparison is based on the criteria of correlation of the propulsive performance nozzles parameter (thrust coefficient) for various operational conditions.

Keywords: Plug Nozzle, thrust coefficient

1. INTRODUCTION

The altitude adaptation is the most attractive feature of the plug nozzle. It is briefly mentioned in the introduction, and is illustrated in Fig.1. It means that the plug nozzle is able to adapt its jet to the surrounding ambient pressure, without considerable thrust loss. The decreasing ambient pressure with increasing altitude requires such an adaptable nozzle, especially for single-stage-to-orbit vehicles. Then, since the nozzle should carry the vehicle over the complete range of the launch, it would experience even worse off-design conditions than multiple-stage vehicles, which may have different nozzle-design conditions for the multiple stages. Therefore, especially for single-stage-to-orbit vehicles the altitude adaptation is an indispensable feature. However, the adaptation is only present in underexpanded condition (Wisse (2005)).

In the Figure 1, Hagemann et al. (1998), summarizes the principle flow phenomena of plug nozzles with full length and truncated central bodies at different off-design (top and bottom) and design (center) pressure ratios that were observed in experiments and numerical simulations. For pressure ratios lower than the design pressure ratio of a plug nozzle with a well-contoured central body, the flow expands near the central plug body without separation, and a system of recompression shocks and expansion waves adapts the exhaust flow to the ambient pressure p_{amb} .

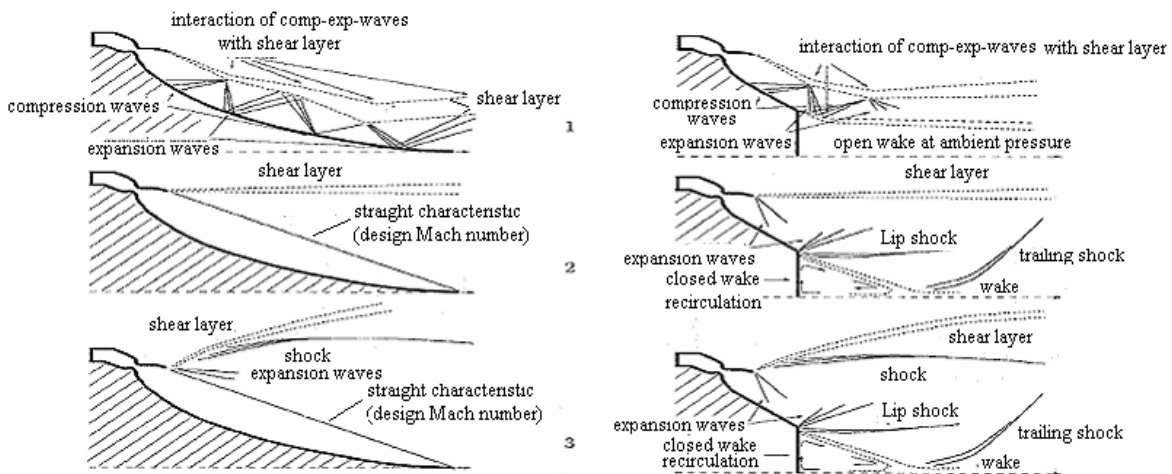


Figure 1 Flow Phenomena of a Plug Nozzle and Truncated Body at Different Pressure ratio p_0/p_{atm} . Off-Design (top, bottom) and Design (center) Pressure Ratio from Hagemann et al, 1998

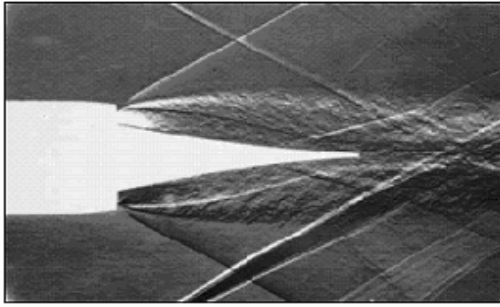
The characteristic barrel-like form with several inflections of the shear-layer results from various interactions of compression and expansion waves with the shear layer, and turbulent diffusion enlarges the shear layer farther

downstream of the throat. The existence of the overexpansion and recompression processes is inferred from up- and down-variations of plug wall pressure profiles observed in various cold-flow tests and numerical simulations. At the design pressure ratio (see Fig. 1, left column, center), the characteristic with the design Mach number should be a straight line emanating to the tip of the central plug body, and the shear layer is parallel to the centerline. However, for circular plug nozzles designed with contouring methods proposed by Angelino and Lee, (1993), no exact one-dimensional exit flow profiles can be achieved, because both methods use the Prandtl–Meyer relations that are only valid for planar flows.

2. STEADY TWO-DIMENSIONAL TRANSONIC FLOW IN PLUG NOZZLES

The determination of the flow pattern in the throat region of a 2-d plug nozzle under choked conditions may be accomplished by applying small perturbation techniques to the equations governing the choked flow Zucrow, (1977) and Wisse (2005). Of the several methods that have been proposed for analyzing the flow field in the throat region of a two-dimensional nozzle, that due to Sauer (1947) is the simplest.

Figures 2 and 3 illustrates schematically the general features of the throat region of a plug nozzle. The contour of the nozzle is symmetrical with respect to the axis x , and it is assumed that the fluid flows in positive direction of the x axis. Figure 3 it is anticipated that the cross-section of the sonic surface, termed the *sonic line*, is a parabola; It is seen in Figure 3 that the sonic line starts from the wall of the nozzle at a point slightly upstream from the *throat* G , the minimum flow area, proceeds downstream, and crosses the centerline of the nozzle at point O . Point O denotes the origin of the coordinate system employed in the analysis due to Sauer (1942). It corresponds to the intersection of the sonic line with the x axis. The location of point O , the distance ϵ downstream from the throat G , is determined from the analysis.



copyright © CNERA 1996-2005 - Tous droits réservés.

Figure 2 Plug Nozzle

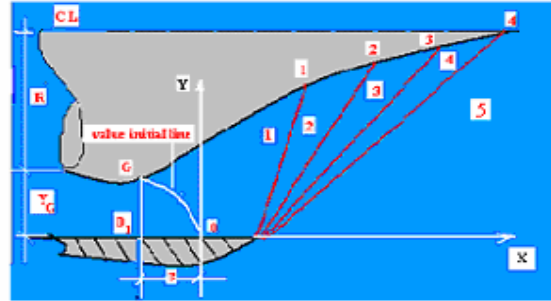


Figure 3 Geometric of the Throat and Coordinate System

for either a two-dimensional planar or axisymmetric irrotational flow, the perturbation equation is Zucrow, (1977):

$$(1 - M_\infty^2)u_x + v_y + \delta \frac{v}{y} = M_\infty^2 (\gamma + 1) \left(\frac{u}{U_\infty} \right) u_x \quad (1)$$

where, $\delta = 0$ for a planar flow and $\delta = 1$ for an axisymmetric flow. Because the flow in the throat region is essentially 1-d and sonic, the undisturbed free-stream velocity U_∞ is chosen as the critical speed of sound a^* ; the corresponding Mach number M_∞ is therefore, equal to unity. Substituting U_∞ and $M_\infty = 1$ into equation (1), obtain:

$$(\gamma + 1) \left(\frac{u}{a} \right) u_x - v_y - \delta \frac{v}{y} = 0 \quad (2)$$

By definition, let $u' = \frac{u}{a}$ and $v' = \frac{v}{a}$, Where u' and v' are termed the *non-dimensional perturbation velocity components*. Introducing u' and v' into equation (2) transforms it to

$$(\gamma + 1)u'u'_x - v'_y - \delta \frac{v'}{y} = 0 \quad (3)$$

Since the flow in the throat region is irrotational, it is possible to define a potential function ϕ for the velocity. Hence, by definition :

$$\Phi = U_{\infty} x + \phi = a^*(x + \phi') \quad (4)$$

where ϕ' is the *nondimensional perturbation velocity potential*. Consequently,

$$\tilde{u} = a^* + u = a^*(1 + u') = \Phi_x = a^*(1 + \phi') \quad (5)$$

$$\tilde{v} = v = a^* v' = \Phi_y = a^* \phi'_y \quad (6)$$

where $u = \phi'_x$ and $v = \phi'_y$. Substituting equations (5) and Equation (6) into equation (3), obtain:

$$(\gamma + 1)\phi'_x \phi'_{xx} - \phi'_{yy} - \delta \frac{\phi'_y}{y} = 0 \quad (7)$$

Equation (7) is the governing equation for the *nondimensional perturbation velocity potential for a transonic flow*. The nonlinear pdf is solved using an approximate method where a power series solution is assumed, with the coefficients of the power series chosen in such a manner that the differential equation and the boundary conditions are satisfied. In case, the velocity potential $\phi'(x, y)$ may be defined by a power series in y , in which the coefficients of $y = f(x)$. Since $u(x, y)$ is an even function of y , $\phi'_x = u$ must be an even function of y ; consequently, only even power of y are included in power series. Thus,

$$\phi(x, y) = \sum_{i=0}^{\infty} f_{2i}(x) y^{2i} = f_0(x) y^0 + f_2(x) y^2 + f_4(x) y^4 + \dots \quad (8)$$

where $y^0 = 1$. The corresponding expressions for terms ϕ'_x , ϕ'_{xx} , ϕ'_y and ϕ'_{yy} are accordingly

$$\phi'_x = f'_0(x) + f'_2(x) y^2 + f'_4(x) y^4 + \dots \quad (9)$$

$$\phi'_{xx} = f''_0(x) + f''_2(x) y^2 + f''_4(x) y^4 + \dots \quad (10)$$

$$\phi'_y = 2f_2(x) y + 4f_4(x) y^3 + \dots \quad (11)$$

$$\phi'_{yy} = 2f_2(x) + 12f_4(x) y^2 + \dots \quad (12)$$

where $f'_0(x)$ denotes $df_0(x)/dx$, and so forth. Substituting the above expressions into equation (7) and rearranging the result, yields the following polynomial in y . Thus,

$$y^0 \left[(\gamma + 1) f'_0 f''_0 - 2f_2 - 2\delta f_2 \right] + y^2 \left[(\gamma + 1) (f'_0 f'_2 + f''_0 f_2) - 12f_4 - 4\delta f_4 \right] + y^4 \dots = 0 \quad (13)$$

Since the polynomial equation (13) must be satisfied for all arbitrary values of x and y , the coefficients of each power of y must be identically zero. Sauer, (1947) truncated the series after the $f_4(x) y^4$ term. Setting the coefficients of y^0 and y^2 equal to zero and solving for $f_2(x)$ and $f_4(x)$ yields:

$$f_2(x) = \frac{(\gamma + 1) f'_0 f''_0}{2(\gamma + \delta)} \quad (14)$$

$$f_4(x) = \frac{(\gamma + 1) (f'_0 f'_2 + f''_0 f_2)_0 f''_0}{4(\gamma + \delta)} \quad (15)$$

This $f_2(x)$ and $f_4(x)$ may be determined from the derivatives of $f_0(x)$. When $y=0$, $u'(x, 0) = f'_0(x)$, where $u'(x, 0)$ defines the nondimensional perturbation velocity distribution along the x axis. Consequently, knowing $u'(x, 0)$, one can

determine $f_2(x)$ and $f_4(x)$ from equations (14) and (15), and, therefore, the flow field. If the axial perturbation velocity distribution is assumed to be linear, $u'(x,0)$ is given by :

$$u'(x,0) = f'_0(x) = \alpha x \quad (16)$$

where α is a constant, termed the coefficient of the linear nondimensional axial perturbation velocity. Substituting equation (16) into equations (14) and (15) gives:

$$f_2(x) = \frac{(\gamma+1)\alpha^2 x}{2(1+\delta)} \quad (17)$$

$$f_4(x) = \frac{(\gamma+1)\alpha^3}{8(1+\delta)(3+\delta)} \quad (18)$$

Substituting equations (17) and (18) into equation (8), yields

$$\phi'(x,y) = f_0(x) + \frac{(\gamma+1)\alpha^2 xy^2}{2(1+\delta)} + \frac{(\gamma+1)\alpha^3 y^4}{8(1+\delta)(3+\delta)} \quad (19)$$

Substituting equation (19) into equations (5) and (6) yields:

$$u'(x,y) = \alpha x + \frac{(\gamma+1)\alpha^2 y^2}{2(1+\delta)} \quad (20)$$

$$v'(x,y) = \frac{(\gamma+1)\alpha^2 xy^2}{2(1+\delta)} + \frac{(\gamma+1)\alpha^3 y^3}{2(1+\delta)(3+\delta)} \quad (21)$$

Equations (20) and (21) yield the *nondimensional perturbation velocities* for a linear axial perturbation velocity distribution. The critical curve where $M=1$ and $(\tilde{u}^2 + \tilde{v}^2) = a^{*2}$ may be determined as follows. First, substitute the definition of nondimensional perturbation velocities. Thus,

$$(\tilde{u}^2 + \tilde{v}^2) = a^{*2} = (a^* + u')^2 + v'^2 = a^{*2} |(1+u')^2 + v'^2| \quad (22)$$

Dividing through by a^{*2} yields:

$$(1+u')^2 + v'^2 = 1 \quad (23)$$

Expanding equation (23) and neglecting powers of u' and v' yields:

$u' = 0$ Consequently, the Critical curve where $M=1$ is established by setting $u' = 0$ in equation (20). Thus,

$$x = -\frac{(\gamma+1)\alpha y^2}{2(1+\delta)} \quad (24)$$

Next, it is necessary to locate the origin of the coordinate system in the nozzle. From Figure 3 it is seen that $\tilde{v} = v = v' = 0$ in $x = \varepsilon$ and $y = y_t$. Substituting those values for x and y into equation (21) yields:

$$\varepsilon = -\frac{(\gamma+1)\alpha y_t^2}{2(3+\delta)} \quad (25)$$

Equation (25) locates the origin of the coordinate system relative to the nozzle throat.

3. Determination of the Nozzle Contour

Figure 4 illustrates the geometric model employed for determining the curvature k of the nozzle wall at the narrowest cross-section (throat). The curvature k is defined as the change in the direction of the tangent to a curve per unit distance along that curve. The radius of curvature at the throat ρ_t is the reciprocal of the curvature k . From Figure 4

$$\tan \tau = \frac{v'}{(1+u')} \equiv v' \quad (26)$$

At the point T, the curvature k is given by

$$k = \frac{1}{\rho_t} = \left(\frac{d(\tan \tau)}{ds} \right)_T = \left(\frac{dv'}{ds} \right)_T \quad (27)$$

To the differentiate dv'/ds one may write

$$\frac{dv'}{ds} = v'_x \left(\frac{dx}{ds} \right) + v'_y \left(\frac{dy}{ds} \right) \quad (28)$$

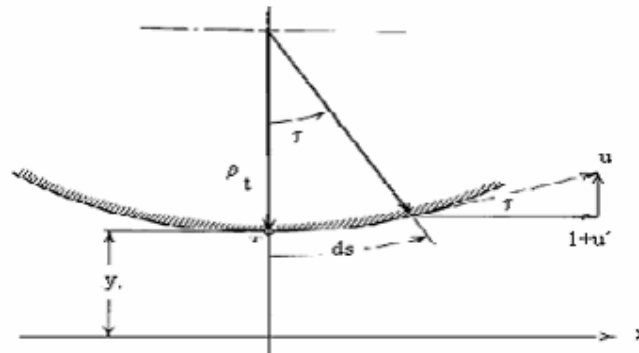


Figure 4 Model for relating the Throat Radius of Curvature to the Flow Field

Consider a nozzle throat with a radius of curvature ρ_t , which is large compared to the throat radius y_t . Hence, $\rho_t \gg y_t$, $(dx/ds) \cong 1$, and $(dy/ds) \cong 0$. Accordingly, equation (28)

$$\frac{dv'}{ds} = v'_x \quad (29)$$

$$\rho_t = \frac{1}{\left| v'_x(x, y) \right|_T} = \frac{1}{v'(\varepsilon, y_t)} \quad (30)$$

From equation (21) v'_x is given by

$$v'_x = \frac{(y+1)\alpha^2 xy^2}{2(1+\delta)} \quad (31)$$

The value of v'_x at the point T, where $x = \varepsilon$ and $y = y_t$, may be determined from equation (31), one obtains the following equation (31). Substituting that result into equation (30), one obtains the following equation for the radius of curvature ρ_t . Thus,

$$\rho_t = \frac{(1 + \delta)}{(\gamma + 1)\alpha^2 y_t} \quad (32)$$

Up to this point it is assumed that the nondimensional axial perturbation velocity $u'(x,0)$ is known, and that a radius of curvature ρ_t for the nozzle wall, as specified by equation (32), is required for obtaining the correct value for $u'(x,0)$. By inverting the interpretation of the preceding results, the value of $u'(x,0)$ may be determined from the geometrical properties of the nozzle throat. Solving equation (32) for α yields:

$$\alpha = \left| \frac{(1 + \delta)}{(\gamma + 1)\rho_t y_t} \right|^{1/2} \quad (33)$$

Substituting equation (33) for α into equation (25) yields the following equation for ε . Thus,

$$\varepsilon = - \frac{y_t}{2(3 + \delta)} \left| \frac{(\gamma + 1)(1 + \delta)}{(\rho_t / y_t)} \right|^{1/2} \quad (34)$$

4. Initial-Value Line for Supersonic Flow Field Calculations

To initiate for the two-dimensional supersonic flow field by the method of characteristics, a line along which $M > 1$ across the entire throat is needed. The sonic line determined by Sauer's Method (1947) is unsuitable because Mach lines from the sonic line intersect the nozzle wall upstream from the throat point T. Because point T was employed as a boundary condition in the evaluation equation (32), the region of the flow field upstream from point T is within the range of influence of point T, and the method of characteristics cannot be initiated from an *initial-value line* that is in range of influence of downstream point. The line where $\tilde{v} = 0$, which is only a slight distance further downstream than the sonic line, may be employed as an *initial-value line* for the method of characteristics. The equation of the line, which is the locus for $\tilde{v} = 0$, is obtained from equation (21) by setting $v' = 0$. Thus,

$$x = - \frac{(\gamma + 1)\alpha y^2}{2(3 + \delta)} \quad (35)$$

The dimensional velocity components \tilde{u} and \tilde{v} may be determined along the line $\tilde{v} = 0$ at any point where x and y are specified. Since the flow is isentropic, the speed of sound a is a known function of the magnitude of the flow velocity V . Knowing V and a , the Mach number M may be calculated. The static thermodynamic properties p, ρ and T may be computed from the stagnation values P, ρ_0 and T and the Mach number M . Hence, all of the gas dynamic properties for the following fluid may be determined along a line that is suitable for initiating a numerical solution by the method of characteristics for the supersonic flow field in the divergence. The mass flow rate for the nozzle may be determined by integrating across any line generated in the throat region by applying the foregoing analysis. Because of the approximations made in the analysis, the accuracy of the results depends to some extent on the choice of the initial-value line to be employed as the initial-value line. The $\tilde{v} = 0$ line (see equation 35) is frequently employed as the initial-value line. The axial thrust developed at the throat of the nozzle may be calculated by integrating the momentum and pressure forces acting across the the initial-value line.

5. Mass Flow rate and Thrust

The differential mass flow rate dm crossing the element of area dA (conventional nozzle) is given

$$dm = \rho V dA = \rho \tilde{u} 2\pi y dy \quad (36)$$

Mass flow rate cross the $v=0$ line. Integrating equation (36) gives

$$\dot{m} = 2\pi \int_0^{y_t} \rho \tilde{u} y dy \quad (37)$$

The actual integration of equation (37) is accomplished by applying Simpson's rule. Dividing the integration interval NPI-1 equal subintervals, yields the following algorithm.

$$\dot{m} = 2\pi \left(\frac{\Delta y}{3} \right) \sum_{i=1}^{NPI} C_i (\rho \tilde{u} y)_i \quad \text{where } C_i = 1, 4, 2, \dots, 2, 4, 1 \text{ and } \Delta y = \frac{\rho_t}{NPI - 1} \quad (38)$$

Thrust across the $v=0$ line. O thrust is the sum of the pressure forces and the momentum flux. From Figure obtain the following expression for the differential thrust acting on dA .

$$dF = 2\pi r p dy + \tilde{u} dm \quad (39)$$

Substituting for dm from equation (39), obtain

$$dF = 2\pi (p + \rho \tilde{u}^2) y dy \quad (40)$$

Integrating equation (40) yields the thrust F. Thus,

$$F = 2\pi \int_0^{y_t} (p + \rho \tilde{u}^2) y dy \quad (41)$$

Equation (41) may be integrated by Simpson's rule. Thus,

$$F = 2\pi \left(\frac{\Delta y}{3} \right) \sum_{i=1}^{NPI} C_i [(p + \rho \tilde{u}^2) y]_i \quad (42)$$

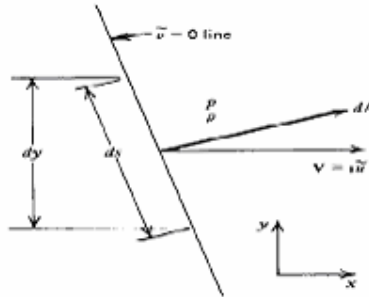


Figure 5 Differential Model for Calculating the Mass Flow Rate and Thrust across the Initial Value Line

The differential mass flow rate dm crossing the element of area dA (Plug nozzle) is given

$$dm = \rho V dA = \rho \tilde{u} 2\pi r dy \quad (43)$$

$$\text{where } r = R + \rho_t \frac{dy}{2} - y \quad (44)$$

Substituting equation (44) into equation (43) and neglecting dy^2 obtain:

$$\dot{m} = 2\pi \int_0^{y_t} \rho u (R + \rho_t - y) dy \quad (45)$$

The actual integration of equation (45) is accomplished by applying Simpson's rule. Dividing the integration interval NPI-1 subintervals yields the following algorithm.

$$\dot{m} = 2\pi \left(\frac{\Delta y}{3} \right) \sum_{i=1}^{NPI} C_i [\rho u (R + y)]_i \quad (46)$$

Similarly for thrust in plug nozzle

$$F = 2\pi \left(\frac{Ay}{3} \right) \sum_{i=1}^{NPI} C_i \left[p + \rho u^2 \right] (R + y)_i \quad (47)$$

To determined flow field or the plug nozzle is admitted isentropic expansion of the jet to the final pressure produces a jet Mach number M, and if γ is the ratio of specific heats, then the angle of refraction is:

$$v = \sqrt{\frac{\gamma+1}{\gamma-1}} \tan^{-1} \sqrt{\frac{\gamma-1}{\gamma+1} (M^2 - 1)} - \tan^{-1} \sqrt{M^2 - 1} \quad (48)$$

Based upon a value of $v = \text{Mach } 1$

In Plug Nozzle of the type shown in Figure 2 all the supersonic expansion occurs externally. It is of course possible, and in many cases advantageous, to piece the total expansion between internal and external expansion Berman,(1960). If assume that the internal expansion is a simple corner expansion, the total expansion angle is the sum of the internal and external expansions:

$$v = (\theta_2 - \theta_1) + (\theta_2 - \theta_3) \quad (49)$$

where v is called the Prandtl-Meyer angle.

6. Solution Method

The basic contour design of the linear plug nozzle is a straightforward process, in principle based on the application of the inviscid irrotational supersonic Prandtl-Meyer flow theory [1908] derived from the Euler equations. The contour is two-dimensional, since the segments are placed linearly next to each other. The determination of the contour surface of the plug nozzle is done of the form where the direction of a frictionless wall is changed by an angle δ at the point where the incident expansion wave impinges on it. No reflected wave is required for causing the streamlines crossing wave to become parallel to the surface. The incident expansion wave ends at the surface because its inclination is such that the reflected wave is neutralized or canceled. I.e., if a weak wave of the angle $\Delta\theta$ incident about the surface of plug nozzle, a reflection wave equal strength must be present of the form to satisfy the boundary condition in surface of the plug nozzle. Similarity obtain all points on the plug nozzle. If we know the position and the properties of a point on the wall, we can easily determine those of the adjacent point until we reach the exit section point. The plug nozzle Figure 3 is designed admitting design pressure in 5 region equal ambient pressure in a determined altitude of the flight. In this case, how the waves splitting the regions are equal families, hence, the waves of the fan expansion of Prandtl-Meyer are equal strength.

$$\Delta\theta = -\Delta v \quad (50)$$

Of the 1 region to 2 region there is one Mach line or characteristic of same family, Thus

$$\begin{aligned} \theta_2 - \theta_1 &= v_2 - v_1 = -\Delta v \\ \theta_2 &= \theta_1 - \Delta v \\ \theta_3 &= \theta_1 - 2\Delta v \\ &\dots\dots\dots \\ \theta_n &= \theta_1 - (n-1)\Delta v \end{aligned} \quad (51)$$

$$\text{Where } \Delta v = \frac{v_5 - v_1}{5}$$

Admitting boundary surface of plug nozzle how a streamline, knowledge the properties and location of the point in the wall of divergent and angle divergence, denoting by 1 region which contain this point and using properties in this region how initial values for determination boundary surface of plug nozzle Figure 6. thus, with the design pressure and the stagnation pressure in combustion chamber specified, obtain through isentropic relations, the number Mach and Prandtl-Meyer angle in the region, hence, also all properties in the region.

$$\begin{aligned}
\alpha_{1,1} &= \arcsen \frac{1}{M_1} + \theta_1 & \alpha_{1,2} &= \theta_1 \\
\alpha_{2,2} &= \arcsen \frac{1}{M_2} + \theta_2 & \text{with } \alpha_{2,2} &= \theta_2 \\
\alpha_{n,1} &= \arcsen \frac{1}{M_n} + \theta_n & \alpha_{n,2} &= \theta_n
\end{aligned}
\tag{52}$$

where $\alpha_{i,j}$ i = region , j = angle α with i,j = 1...n

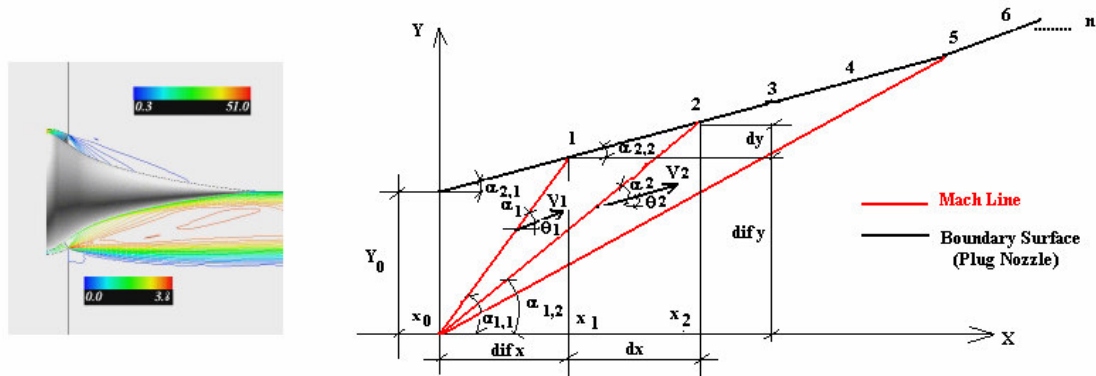


Figure 6 a): Contour plots of pressure (upper half) and Mach number (lower half) distributions (Pressure Ratio 71) Ito et al (1999) b) Mach Lines

$$dx = \frac{dix \cdot \tan \alpha_{2,1} - dify}{\tan \alpha_{2,2} - \tan \alpha_{2,1}}
\tag{53}$$

Thus, knowing all coordinate and angle of the points on wall with the axis line, determine the ordinate Y_{cc} of the radius cone of the plug nozzle. Figure 6b

$$y_{cc} = (x_1 - x_0) \tan \theta_1 + (x_2 - x_1) \tan \theta_2 + \dots
\tag{54}$$

Equation (54) is applicable for all n Mach lines.

Thrust on Plug Nozzle

Variation of the Thrust on plug nozzle, Pires, (1996) is given by:

$$DF = \pi [(P_w - P_{amb}) (R - y_w) + (P_i - P_{amb}) (R - y_i)] y_i - y_w
\tag{55}$$

7. Result

Developed computational codes in Fortran 77 Pires, (1996), Lee (1963 and 1964) with objective of analyze different nozzle concepts with improvements in performance as compared to conventional nozzle achieved by altitude adaptation and, thus, minimizing losses caused by over- or underexpansion. The plug nozzle provides, at least theoretically a continuous altitude adaptation up to their geometrical area ratio. The Figure 8 shows the thrust coefficient (C_F) of the Plug Nozzle plotted against the pressure ratio. The solid red line denotes the ideal thrust coefficient and the dashed green line the theoretical C_F of the conventional nozzle. In the low pressure ratio region, the standard nozzle not produce as much thrust as the plug nozzle (blue line). That is the reason for higher performance of the plug nozzle at lower altitudes. The plug nozzle operates at nearly peak thrust efficiency in the wide range of the pressure ratio than the conventional nozzle type Bell.

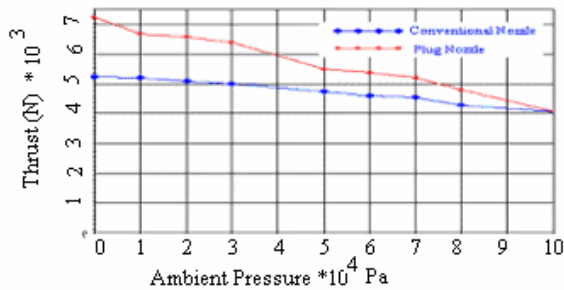


Figure 7 Ambient Pressure (Pa) versus Thrust (N)

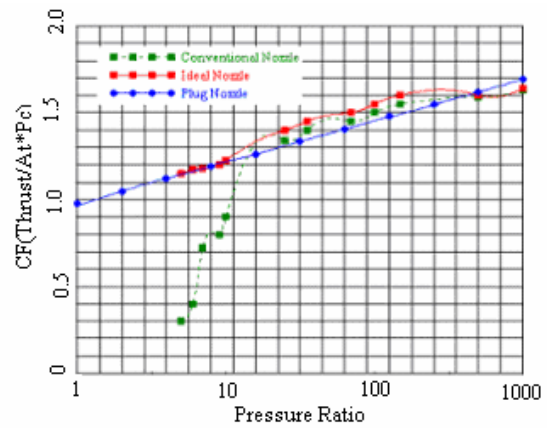


Figure 8 Pressure Ratio Versus Thrust Coefficient

8. Conclusion

The flow structure and the performance of the plug nozzle are numerically investigated. The results clearly showed the main advantages of the plug nozzle. Conventional Bell-type rocket nozzles, which are in use in practically all of today's rockets, limit the overall engine performance during the ascent of the launcher owing to their fixed geometry. Significant performance losses are induced during the off-design operation of the nozzles, when the flow is overexpanded during low-altitude operation with ambient pressures higher than the nozzle exit pressure, or underexpanded during high-altitude operation with ambient pressures lower than the nozzle exit pressure. In the case of overexpanded flow, oblique shocks emanating into the flow field adapt the exhaust flow to the ambient pressure. Further downstream, a system of shocks and expansion waves leads to the characteristic barrel-like form of the exhaust flow. In contrast, the underexpansion of the flow results in a further expansion of the exhaust gases behind the rocket. Off-design operations with either overexpanded or underexpanded flow result in significant performance gains from the adaptation of the exhaust flow to the ambient pressure. Special attention is then given to altitude-adaptive nozzle concepts, which have recently received new interest in the space industry. In general, flow adaptation induces shocks and expansion waves, which result in exit properties that are quite different from idealized one-dimensional assumptions. The consideration of derived performance characteristics in launcher and trajectory optimization calculations reveal significant payload gains at least for some of these advanced nozzle concepts.

9. REFERENCES

- Angelino, G., July 1963, "Theoretical and Experimental Investigations of the Design and Performance of a Plug Type Nozzle," NASA TN-12.
- Back L.H., et al, September, 1965 "Comparison of Measured and Predicted Flows through Conical Supersonic Nozzles, with Emphasis on the Transonic Region", Journal of American Institute of Aeronautics and Astronautics, Vol.3, No.9, pp 1606-1614.
- Berman, K. and Crimp, J.F.W., 1960 "Performance of Plug-Type Rocket Exhaust Nozzles" ARS Solid Propellant Rocket Research Conference, Princeton, N.J.
- Ito T. et al. "Computations of the Axisymmetric Plug Nozzle Flow Fields- Flow Structures and Thrust Performance - 17th AIAA Applied Aerodynamics Conference Jun 28- Jul 1. 1999 Norfolk, Virginia pp 768-778
- Lee C., and Thompson D., 1964 "Fortran Program for Plug Nozzle Design", NASA TM X-53019
- Manski, D., and Hagemann, G., 1996 "Influence of Rocket Design Parameters on Engine Nozzle Efficiencies," *Journal of Propulsion and Power*, Vol. 12, No. 1, pp. 41-47.
- T. Meyer, 1908 "Über zweidimensionale Bewegungsvorgänge in einem Gas, das mit Überschallgeschwindigkeit strömt, Ph.D. thesis, Göttingen.
- Pires, M., 1996 "Escoamento Supersonico em um Expansor Convergente com Corpo Central"- Master Thesis - Instituto Militar de Engenharia-IME.
- Sauer, R. 1947 "General Characteristics of the Flow through Nozzles at Near Critical Speeds" NACA TM 1147.
- Wisse, M.E.N., 2005 "An Asymptotic Analysis of Compressible Base Flow and the Implementation into Linear Plug Nozzles" Ph.D. Thesis, Technische Universiteit Delft, Netherlands.
- Zucrow M.J., Holmann J.D., 1977 "Gas Dynamics", Vols 1 and 2 John Wiley and Sons
- Zucrow M.J., Holmann J.D., 1958 "Aircraft and Missile Propulsion, Vol.1. Wiley, New York.

10. RESPONSIBILITY NOTICE

The authors are the only responsible for the printed material included in this paper.